THE ASTROPHYSICAL JOURNAL, 481:795–799, 1997 June 1

THE AMOUNT OF CH PRODUCED DURING CH^+ SYNTHESIS IN INTERSTELLAR CLOUDS[1]

S. R. FEDERMAN
Department of Physics and Astronomy, University of Toledo, Toledo, OH 43606
D. E. WELTY
Astronomy and Astrophysics Center, University of Chicago, Chicago, IL 60637
AND
JASON A. CARDELLI[2]
Department of Astronomy and Astrophysics, Villanova University, Villanova, PA 19085
Received 1996 October 10; accepted 1996 December 30

ABSTRACT

A particularly useful constraint for models of CH^+ formation in interstellar clouds is knowledge of the amount of CH associated with CH^+ synthesis. For lines of sight with no detectable CN absorption, this column of CH can be inferred through a combined analysis of C I excitation and simplified chemical models. The approach is applied to data for two lines of sight, those toward 23 Ori and β^1 Sco, for which $N(CH)/N(CH^+) \leq 0.40$.

Subject headings: ISM: abundances — ISM: molecules — molecular processes

1. INTRODUCTION

While simple gas-phase chemical models can apparently account for the observed abundances of CH, C_2, and CN in diffuse and translucent interstellar clouds, the routes for CH^+ synthesis remain elusive. The most promising theoretical models rely on nonequilibrium processes for which the endothermic reaction $C^+ + H_2 \rightarrow CH^+ + H$ can proceed efficiently. These processes include hydrodynamic shocks (Elitzur & Watson 1978), magnetohydrodynamic shocks (Draine & Katz 1986; Pineau des Forêts et al. 1986), cloud boundary layers (Duley et al. 1992; Falgarone, Pineau des Foréts, & Roueff 1995; Hogerheijde et al. 1995), and propagating Alfvén waves (Federman et al. 1996).

Since different chemical species can be formed in different physical regions along a given line of sight, it is important to determine the relative chemical abundances *in the region of* CH^+ *synthesis* to test the various proposed models. The species CN and CH^+, for example, are likely to be found in very different regions. The CN molecule is produced in observable quantities only after significant amounts of precursor molecules, such as CH and C_2, are available (e.g., Federman, Danks, & Lambert 1984; Federman et al. 1994), and so traces moderately dense gas. The CH^+ molecular ion, on the other hand, is found primarily in regions of lower density, since it is rapidly destroyed at high densities. The distinction between these two species is clearly shown by the inverse relationship found between their total line-of-sight column densities when each is normalized by $N(CH)$ (Cardelli et al. 1990).

The CH radical can be present in both high- and low-density gas. It can be produced early in the chemical sequence occurring in moderately dense gas via $C^+ + H_2 \rightarrow CH_2^+ + h\nu$ (e.g., Federman et al. 1984), or it can be a product of CH^+ synthesis in lower density material (e.g., Draine & Katz 1986). The distinction between the two sources of CH has not been considered in most theoretical efforts on cloud envelopes, however. Typically, the total observed column of CH is used as a constraint in modeling the chemistry of moderately dense gas that leads to CN production, but recent evidence suggests that not all the CH should be used in such models. Federman et al. (1994) found a much stronger correlation between $N(C_2)$ and $N(CN)$ than between either of these columns with $N(CH)$ and suggested that CH is more widely distributed along the lines of sight than are C_2 and CN—i.e., that there is some CH that is not associated with C_2 or CN. In this study, we assume that this additional CH arises primarily from the synthesis of CH^+.

It has generally been difficult to disentangle the amount of CH formed along with CH^+ from the amount associated with CN from line profile information alone. Most currently available spectra of CH, CN, and CH^+, obtained at resolutions of 3–6 km s^{-1} (FWHM), show no discernible difference in velocity between the three species (e.g., Gredel, van Dishoeck, & Black 1993). Higher resolution (0.3–0.6 km s^{-1}) spectra, however, often reveal differences in the respective line profiles, suggesting that multiple components with different relative abundances of the three molecules are likely to be present in many cases (Crane, Lambert, & Sheffer 1995; Crawford 1995). Roughly two-thirds of the individual components identified in the Crane et al. survey of CH and CH^+ were detected in both species, with similar line widths for the corresponding components suggesting physical association of the two. For a smaller sample, Crawford (1995), on the other hand, found CH^+ components to be systematically broader than their counterparts in CH, which would imply some difference in distribution. The few components detected only in CH had systematically smaller line widths than the others and might plausibly be associated with components seen in CN for cases where comparable high-resolution spectra of CN have been obtained. Even the narrowest of these molecular components is wider than would be expected from thermal broadening alone, if the gas is cool. We note, however, that spectra capable of resolving individual component line widths may not reveal all the components present (and thus

[1] Based on observations obtained with the NASA/ESA *Hubble Space Telescope* through the Space Telescope Science Institute, which is operated by the Association of Universities for Research in Astronomy, Inc., under NASA contract NAS 5-26555.
[2] Deceased.

TABLE 1

DATA FOR C I ANALYSIS

Parameter	23 Ori	β^1 Sco[a]
$N(0)$ (cm^{-2}).....	$(8.5 \pm 1.0) \times 10^{14}$	$(2.10 \pm 0.32) \times 10^{14}$
$N(1)$ (cm^{-2}).....	$(9.0 \pm 2.0) \times 10^{13}$	$(3.61 \pm 0.21) \times 10^{13}$
$N(2)$ (cm^{-2}).....	$(1.4 \pm 0.3) \times 10^{13}$	$(1.66 \pm 0.19) \times 10^{13}$
x(H)	0.90	0.58
x(He)	0.10	0.10
x(o$-H_2$).....	0.0	0.18
x(p$-H_2$).....	0.0	0.14
T (K).....	65–150	77–103

[a] Snow & Jenkins 1980 found $N(0) = (0.79–1.4) \times 10^{14}$, $N(1) = (2.6–4.2) \times 10^{13}$, and $N(2) = (2.1–3.5) \times 10^{13}$; Jenkins et al. 1983 found $N(0) = (0.95–1.7) \times 10^{14}$, $N(1) = (2.3–3.8) \times 10^{13}$, and $N(2) = (0.89–2.2) \times 10^{13}$.

may not yield accurate widths) when the individual components are relatively weak, intrinsically broad, and/or closely blended.

There are a number of lines of sight (or individual components) with CH and CH^+ detections and with fairly stringent upper limits on the amount of CN. For example, the high-resolution spectra of the molecular lines toward ζ Oph have revealed a distinct broad component of CH which appears to be associated with CH^+ but not with CN (Lambert, Sheffer, & Crane 1990; Crawford et al. 1994). While we expect that such cases are indicative of somewhat lower gas densities, the available upper limits on CN do not by themselves necessarily imply that all the observed CH is associated with CH^+. In this paper, we estimate the density in the main absorbing components toward the stars 23 Ori and β^1 Sco via an analysis of the C I fine-structure equilibrium. For these two lines of sight, the low inferred densities suggest that the observed CH is in fact associated with CH^+ rather than with (undetected) CN.

2. OBSERVATIONAL DATA

As a part of other programs, ultraviolet data on C I lines toward the stars 23 Ori and β^1 Sco were acquired with the Goddard High Resolution Spectrograph (GHRS) on the *Hubble Space Telescope* (*HST*). Most of the accessible C I lines were observed toward 23 Ori, using the Echelle A grating for the multiplet at 1260 Å and the G160M grating for the others. For β^1 Sco, the G160M was used to measure the lines in the wavelength intervals 1155–1160 Å and 1185–1200 Å. C I equivalent widths for β^1 Sco obtained with the *Copernicus* satellite (Snow & Jenkins 1980; Jenkins, Jura, & Loewenstein 1983) were also included in our analysis. The procedures for reduction of the GHRS data can be found in Federman et al. (1995) and Welty et al. (1997); they will not be repeated here. We have used the *f*-values compiled by Morton (1991) and those derived from astronomical curves of growth (Zsargo, Federman, & Cardelli 1997) in our profile-fitting (23 Ori) and curve-of-growth (β^1 Sco) analyses. The resulting column densities for C I are listed in Table 1.

3. ANALYSIS AND RESULTS

3.1. *Carbon Excitation*

The local gas density can be estimated through analysis of the distribution of fine-structure levels in the ground state of C I (e.g., Jenkins et al. 1983), if the temperature can also be obtained (e.g., from the $J = 0$ and 1 rotational levels of H_2; Savage et al. 1977). Our statistical equilibrium analysis of C I is similar to the one performed by Lambert et al. (1994) for the line of sight toward ζ Oph. In particular, the rates for collisional excitation for atomic hydrogen are from Launay & Roueff (1977), for ortho- and para-hydrogen, from Schröder et al. (1991), and for He, from Lavendy, Robbe, & Roueff (1991) and Staemmler & Flower (1991). Ultraviolet pumping (Jenkins & Shaya 1979) is also included, but it plays a minor role. The necessary observational parameters used in our analysis—the column density of C I in each fine-structure level, $N(J)$, the fractional amounts of H, He, and ortho- and para-H_2, x(X), and the temperature—are listed in Table 1. Earlier determinations of the C I column densities based on *Copernicus* spectra appear as notes to the table.

The statistical equilibrium calculation yielded values for gas density, n, and temperature, T, consistent with the observed column density ratios, $N(2)/N(0)$ and $N(1)/N(0)$. The curves showing the allowed ($\pm 2\ \sigma$) ranges in n and T are displayed in Figure 1. The values for $T_{10}(H_2)$ derived from H_2 measurements are indicated by short-dashed lines. For the gas toward 23 Ori, both ratios give comparable results, and the derived range in n for $T = T_{10}(H_2) \sim 120$ K is 10–20 cm^{-3}. For β^1 Sco, the curves for $N(1)/N(0)$ always yield smaller densities than those for $N(2)/N(0)$. For $T = T_{10}(H_2) \sim 90$ K, the acceptable values for n probably lie between 40 and 80 cm^{-3}. Jenkins et al. (1983) noted this

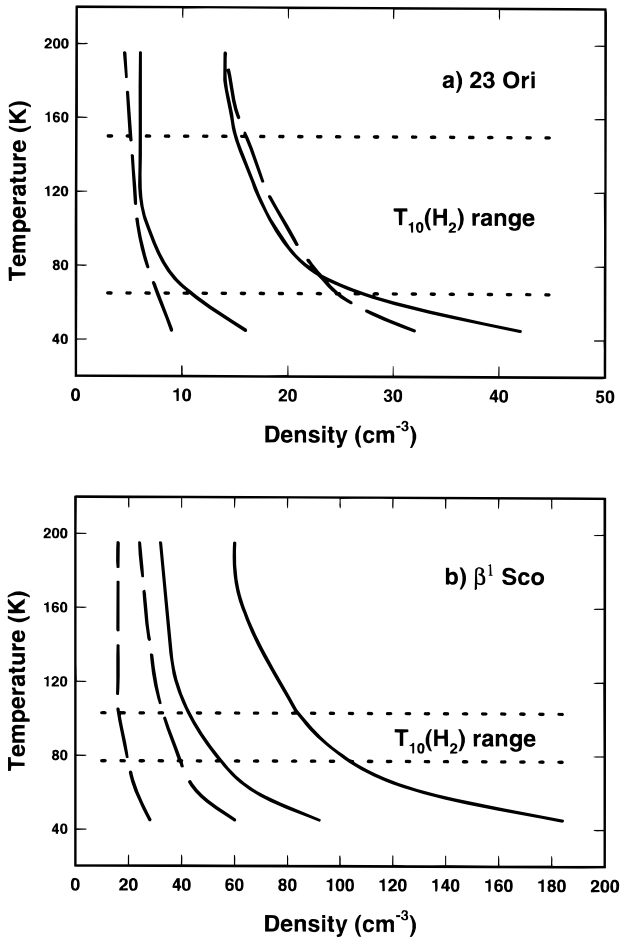

FIG. 1.—Results of analyzing the C I fine-structure levels. Solid curves show the acceptable range of n and T from the $N(2)/N(0)$ ratio, while long-dashed lines show the range for the $N(1)/N(0)$ ratio. The short-dashed lines represent the allowed H_2 excitation temperatures.

inconsistency in their analysis based on *Copernicus* data; several different regions, at similar velocities but with slightly different properties, may be present. For comparison, Lambert et al. (1994) found densities between 100 and 200 cm^{-3} for the molecule-rich gas toward ζ Oph.

3.2. *Chemical Analysis*

The simplified chemical analysis is based on analytic expressions for column densities that are derived from rate equations assuming no dependence on time (e.g., Federman et al. 1984, 1994). These expressions incorporate the most important processes, and our previous work indicated that the expressions reproduce the observational data on CH, C_2, and CN, as well as results from more detailed computations. Here we are mainly interested in the equation for CH, which is

$$N(\mathrm{CH}) = \frac{0.67 k_1\, x(\mathrm{C}^+) N(\mathrm{H}_2) n}{G(\mathrm{CH})} . \quad (1)$$

Destruction via reactions with C^+, N, and O is of minor importance relative to photodissociation along these lines of sight. In this and subsequent equations, k_i is the rate constant for reaction i, x(X) is the fractional abundance relative to total hydrogen nuclei for species X, n is the gas density $[n(\mathrm{H}) + 2n(\mathrm{H}_2)]$, and G(X) is the photodissociation rate for species X, including attenuation of ultraviolet radiation by grains. The attenuation can be approximated by $\tau_{uv} = 2A_V$ when forward scattering is taken into account (e.g., Federman et al. 1994). A comparison between the densities derived from C I excitation and this equilibrium chemical scheme can be made by inverting equation (1) and solving for n:

$$n = \frac{G(\mathrm{CH}) N(\mathrm{CH})}{0.67 k_1\, x(\mathrm{C}^+) N(\mathrm{H}_2)} . \quad (2)$$

As a check on our results for CH, we compared available upper limits for $N(C_2)$ and N(CN) with the following two expressions (Federman et al. 1994):

$$N(\mathrm{C}_2) = \frac{k_2\, x(\mathrm{C}^+) n N(\mathrm{CH})}{G(\mathrm{C}_2)} , \quad (3)$$

$$N(\mathrm{CN}) = \frac{[k_3\, x(\mathrm{N}) N(\mathrm{C}_2) + k_4\, x(\mathrm{N}) N(\mathrm{CH}) + k_5\, x(\mathrm{C}^+) N(\mathrm{NH})] n}{G(\mathrm{CN})} . \quad (4)$$

The column density for NH is estimated by scaling the results of Meyer & Roth (1991) for the gas toward ζ Per by the ratio of CH columns. Further simplifications come from combining equations (2) and (3) and equations (2) and (4) so that

$$N(\mathrm{C}_2) = \left(\frac{1}{0.67}\right)\left(\frac{k_2}{k_1}\right)\left[\frac{G(\mathrm{CH})}{G(\mathrm{C}_2)}\right]\left[\frac{N(\mathrm{CH})}{N(\mathrm{H}_2)}\right] N(\mathrm{CH}) , \quad (5)$$

$$N(\mathrm{CN}) = \left(\frac{1}{0.67}\right)\left[\frac{k_4\, x(\mathrm{N}) + \beta k_5\, x(\mathrm{C}^+)}{k_1\, x(\mathrm{C}^+)}\right] \times \left[\frac{G(\mathrm{CH})}{G(\mathrm{CN})}\right]\left[\frac{N(\mathrm{CH})}{N(\mathrm{H}_2)}\right] N(\mathrm{CH}) . \quad (6)$$

TABLE 2

CHEMICAL DATA

Reaction	Rate/Rate Constant	Value[a]
$C^+ + H_2 \rightarrow CH_2^+ + h\nu$	k_1	1.0×10^{-16}
$C^+ + CH \rightarrow C_2^+ + H$	k_2	3.0×10^{-10}
$C_2 + N \rightarrow CN + C$	k_3	$1.7 \times 10^{-11}(T/300)^{0.5}$
$CH + N \rightarrow CN + H$	k_4	$2.0 \times 10^{-11}(T/300)^{0.5}$
$C^+ + NH \rightarrow$ all	k_5	2.8×10^{-10}
$CH + h\nu \rightarrow C + H$	G(CH)	$1.3 \times 10^{-9} \exp(-\tau_{uv})$
$C_2 + h\nu \rightarrow 2C$	$G(C_2)$	$2.0 \times 10^{-10} \exp(-\tau_{uv})$
$CN + h\nu \rightarrow C + N$	G(CN)	$1.0 \times 10^{-10} \exp(-\tau_{uv})$

[a] The rate constants k_i have units of $cm^3\ s^{-1}$, and rates $G(X)$ have units of s^{-1}.

In deriving equation (6), we have neglected the term in equation (4) with $N(C_2)$ and have defined $\beta = N(\mathrm{NH})/N(\mathrm{CH})$; toward ζ Per, $\beta = 0.045$. Table 2 gives the various rate constants and photodissociation rates, as described in detail by Federman et al. (1994). Table 3 lists the optical depth at 1000 Å due to grain absorption and scattering, the fractional abundances of C^+, N, and O, and the necessary column densities. The fractional abundances come from our analyses of *HST* data presented elsewhere (e.g., Cardelli et al. 1996; Welty et al. 1997). The molecular data on carbon-bearing molecules toward β^1 Sco come from Lambert, Sheffer, & Federman (1995), the compilation in Federman et al. (1994), and, for CH^+, from Federman (1982) and Lambert & Danks (1986); the data for 23 Ori are from Welty et al. (1997), who, for CH^+, agree with the results of Federman (1982) and Lambert & Danks (1986). [Note that the value for N(CH) toward 23 Ori in Crane et al. 1995 is too large; P. Crane 1996, private communication.]

The use of equation (2) with the data compiled in Tables 2 and 3 yields estimates for n under the assumption that the observed columns of CH are *not* associated with the non-equilibrium chemistry required for CH^+ production. For both lines of sight, the resultant density is much larger than that found from C I excitation ($n \leq 80\ cm^{-3}$): $n \approx 10^5\ cm^{-3}$ for 23 Ori and $n \approx 10^3\ cm^{-3}$ for β^1 Sco. The very large estimate for the gas toward 23 Ori arises because N(CH) is moderately high while $N(H_2)$ is very low. The differences in n are larger than can be accounted for by plausible uncertainties in the various input parameters. As a test of the reasonableness of this approach, we also derived n toward ζ Oph from the observed column of CH not associated with CH^+ (Crane et al. 1995). We obtained $n \sim 600\ cm^{-3}$, which compares favorably with the values $n \sim 100$–$200\ cm^{-3}$ esti-

TABLE 3

ADDITIONAL DATA FOR CHEMICAL ANALYSIS

Parameter	23 Ori	β^1 Sco
τ_{uv}	0.68	1.24
$x(C^+)$	2.8×10^{-4}	1.38×10^{-4}
x(N)	8.0×10^{-5}	6.46×10^{-5}
x(O)	3.6×10^{-4}	2.82×10^{-4}
N(CH) (cm^{-2})	5.1×10^{12}	1.9×10^{12}
$N(H_2)$ (cm^{-2})	2.0×10^{18}	6.7×10^{19}
$N(H) + 2N(H_2)$ (cm^{-2})	5.0×10^{20}	1.3×10^{21}
$N(CH^+)$ (cm^{-2})	1.3×10^{13}	5.4×10^{12}
N(CN) (cm^{-2})	$\leq 3.7 \times 10^{11}$	$\leq 1.3 \times 10^{11}$
$N(C_2)$ (cm^{-2})	...	$\leq 1.2 \times 10^{12}$

mated from C I excitation (Lambert et al. 1994) and $n \sim 400$ cm^{-3} from carbon chemistry (Federman et al. 1994).

Given N(CH), we can use equations (5) and (6) to predict the column densities of C_2 and CN under the assumption that the three species are products of equilibrium chemistry. For 23 Ori, the predicted N(CN) is 2 orders of magnitude larger than the observed upper limit. For β^1 Sco, the predicted column densities are larger than the observed upper limits by 30%–50%. Conversely, given the observed upper limits for C_2 and CN, we can derive upper limits for the amount of CH that could be due to equilibrium chemistry (i.e., not associated with CH^+). For 23 Ori, we obtain $N(\mathrm{CH}) \leq 4.7 \times 10^{11}$ cm^{-2}, i.e., less than 10% of the observed CH. For β^1 Sco, the upper limits for both C_2 and CN imply $N(\mathrm{CH}) \leq 1.6 \times 10^{12}$ cm^{-2}, or less than about 85% of the observed CH. While estimates derived from equations (4) and (6) are somewhat uncertain because of the assumption that N(NH) scales with N(CH), we note that (1) for β^1 Sco the upper limits on N(CH) obtained from C_2 and CN are almost identical, and that (2) even if N(NH) were much smaller toward 23 Ori than assumed in the above calculation, we would still find that less than 25% of the observed CH could be associated with C_2 and CN. We thus conclude that most of the CH toward 23 Ori, and a significant fraction of the CH toward β^1 Sco, is likely to have been produced via whatever nonequilibrium processes are responsible for the observed CH^+.

4. DISCUSSION

There are now CH data for three lines of sight, including ζ Oph, useful in constraining models of CH^+ synthesis via nonequilibrium processes. In all three cases, the line widths seem consistent with an association between the CH and CH^+ absorption, with b-values typically 2–3 km s^{-1} for both. For the line of sight toward ζ Oph, the broad component in CH is seen at the same velocity as the single broad component in CH^+ (Lambert et al. 1990; Crawford et al. 1994). The ultra–high-resolution spectra of Crane et al. (1995) and spectra we obtained at resolutions of 1.3–2.5 km s^{-1} reveal relatively broad CH and CH^+ absorption features at similar velocities toward 23 Ori and β^1 Sco as well. For the gas toward β^1 Sco, the b-values are $\sim$2.5 km s^{-1} for both molecules. Similar widths are found for the CH and CH^+ lines toward 23 Ori, though part of the broadening in this case is likely due to the presence of two components of comparable strength separated by $\sim$2.1 km s^{-1} that are seen in the high-resolution profiles of various atomic lines (Welty et al. 1997).

The observed column densities of CH and CH^+ for 23 Ori and β^1 Sco are listed in Table 3; for ζ Oph we have $N(\mathrm{CH}) = 1.1 \times 10^{13}$ cm^{-2} and $N(\mathrm{CH}^+) = 3.0 \times 10^{13}$ cm^{-2} (Lambert et al. 1990; Crawford et al. 1994). Although the number of lines of sight is limited, for a range of a factor of 10 in $N(\mathrm{CH}^+)$ the ratio $N(\mathrm{CH})/N(\mathrm{CH}^+)$ is similar for the three lines of sight, namely 0.35–0.40 (with a lower limit of 0.06 for β^1 Sco, given the various uncertainties). The similar ratios suggest that whatever the amount of CH^+ synthesized via nonequilibrium processes in these lines of sight, an amount of CH that is a constant fraction of the amount of CH^+ is also formed. If this result were true in general, then we would expect some minimum amount of CH to be present whenever CH^+ is detected. There are cases (e.g., several Pleiades stars), however, where CH^+ has been detected with fairly stringent upper limits on CH; a different process may be responsible for the CH^+ in such lines of sight. Analyses like those presented here, but for other lines of sight, are needed to assess how narrow a range in $N(\mathrm{CH})/N(\mathrm{CH}^+)$ is generally present in the region of CH^+ synthesis. Other lines of sight in the survey of Crane et al. (1995), especially those with broad CH components, would be good candidates for further investigation of the relationship between CH and CH^+ production.

In conclusion, our analysis, based both on comparing densities derived from C I excitation with those corresponding to equilibrium chemistry and on comparing relative chemical abundances, suggests that the amount of CH associated with CH^+ is $\leq$40% of the amount of CH^+. These results indicate that modeling efforts should focus on cases where the total gas density is low ($n \leq 50$ cm^{-3}) and where the fraction of hydrogen in molecular form is considerably less than 1. Other constraints on the mechanism(s) of CH^+ formation include the strong relationship between $N(\mathrm{CH}^+)$ and the amount of H_2 in excited rotational levels (Frisch & Jura 1980; Lambert & Danks 1986) and the apparent lack of correspondence between $N(\mathrm{CH}^+)$ and N(OH) (e.g., Federman et al. 1996). The first additional constraint suggests that the excited H_2 rotational levels are populated via processes in the material where CH^+ is formed, while the second seems to indicate that hot gas, which occurs in hydrodynamic shocks and cloud boundary layers, is not responsible for CH^+ production. In particular, since OH can be produced via an endothermic reaction analogous to that for CH^+, one would expect a correspondence between $N(\mathrm{CH}^+)$ and N(OH) that is not seen in material toward stars in Per OB2. If the gas were not hot, OH would be produced in observable quantities solely through ion-molecule reactions and some nonequilibrium effect would be required to drive the production of CH^+ through $C^+ + H_2 \rightarrow CH^+ + H$. The general lack of significant velocity differences between CH and CH^+ components suggests that shocks are not the primary source of CH^+. These pieces, taken together, provide constraints for improved models of CH^+ synthesis.

D. E. W. acknowledges support from NASA LTSA grant NAG 5-3228 and through grant GO-2251.01-87A from the Space Telescope Science Institute, which is operated by the Association of Universities for Research in Astronomy, Inc., under NASA contract NAS 5-26555. S. R. F. thanks the Department of Astronomy at the University of Wisconsin-Madison for hospitality during the early phases of this project.

REFERENCES

Cardelli, J. A., Meyer, D. M., Jura, M., & Savage, B. D. 1996, ApJ, 467, 334
Cardelli, J. A., Suntzeff, N. B., Edgar, R. J., & Savage, B. D. 1990, ApJ, 362, 551
Crane, P., Lambert, D. L., & Sheffer, Y. 1995, ApJS, 99, 107
Crawford, I. A. 1995, MNRAS, 277, 458
Crawford, I. A., Barlow, M. J., Diego, F., & Spyromilio, J. 1994, MNRAS, 266, 903
Draine, B. T., & Katz, N. 1986, ApJ, 306, 655
Duley, W. W., Hartquist, T. W., Sternberg, A., Wagenblast, R., & Williams, D. A. 1992, MNRAS, 255, 463
Elitzur, M., & Watson, W. D. 1978, ApJ, 222, L141
Falgarone, E., Pineau des Forêts, G., & Roueff, E. 1995, A&A, 300, 870
Federman, S. R. 1982, ApJ, 257, 125
Federman, S. R., Cardelli, J. A., van Dishoeck, E. F., Lambert, D. L., & Black, J. H. 1995, ApJ, 445, 325
Federman, S. R., Danks, A. C., & Lambert, D. L. 1984, ApJ, 287, 219

Federman, S. R., Rawlings, J. M. C., Taylor, S. D., & Williams, D. A. 1996, MNRAS, 279, L41
Federman, S. R., Strom, C. J., Lambert, D. L., Cardelli, J. A., Smith, V. V., & Joseph, C. L. 1994, ApJ, 424, 772
Frisch, P. C., & Jura, M. 1980, ApJ, 242, 560
Gredel, R., van Dishoeck, E. F., & Black, J. H. 1993, A&A, 269, 477
Hogerheijde, M. R., de Geus, E. J., Spaans, M., van Langevelde, H. J., & van Dishoeck, E. F. 1995, ApJ, 441, L93
Jenkins, E. B., Jura, M., & Loewenstein, M. 1983, ApJ, 270, 88
Jenkins, E. B., & Shaya, E. J. 1979, ApJ, 231, 55
Lambert, D. L., & Danks, A. C. 1986, ApJ, 303, 401
Lambert, D. L., Sheffer, Y., & Crane, P. 1990, ApJ, 359, L19
Lambert, D. L., Sheffer, Y., & Federman, S. R. 1995, ApJ, 438, 740
Lambert, D. L., Sheffer, Y., Gilliland, R. L., & Federman, S. R. 1994, ApJ, 420, 756
Launay, J. M., & Roueff, E. 1977, A&A, 56, 289
Lavendy, H., Robbe, J. M., & Roueff, E. 1991, A&A, 241, 317
Meyer, D. M., & Roth, K. C. 1991, ApJ, 376, L49
Morton, D. C. 1991, ApJS, 77, 119
Pineau des Forêts, G., Flower, D. R., Hartquist, T. W., & Dalgarno, A. 1986, MNRAS, 220, 801
Savage, B. D., Bohlin, R. C., Drake, J. F., & Budich, W. D. 1977, ApJ, 216, 291
Schröder, K., Staemmler, V., Smith, M. D., Flower, D. R., & Jaquet, R. 1991, J. Phys. B, 24, 2487
Snow, T. P., & Jenkins, E. B. 1980, ApJ, 241, 161
Staemmler, V., & Flower, D. R. 1991, J. Phys. B, 24, 2343
Welty, D. E., Hobbs, L. M., Lauroesch, J. T., Morton, D. C., Spitzer, L., & York, D. G. 1997, in preparation
Zsargo, J., Federman, S. R., & Cardelli, J. A. 1997, ApJ, in press